

MODELLING THE EFFECT OF MATERIAL ANISOTROPY ON IMPACTS INTO LAYERED

TARGETS. R. T. Hopkins¹, G. S. Collins², G. R. Osinski^{1,3}, E. A. Silber¹. ¹Dept. Physics and Astronomy & Centre for Planetary Science And Exploration, Universtiy of Western Ontario, London, Ontario, CANADA, N6A 5B7, ²Dept. Earth Science and Engineering, Imperial College, London, UK, SW7 2BP, ³Dept. Earth Sciences, Universtiy of Western Ontario, London, Ontario, CANADA, N6A 5B7. (rhopkin8@uwo.ca)

Introduction: The formation and final morphology of hypervelocity impact craters is strongly dependant on the composition and structure of the target planetary surface. On Earth, over two-thirds of the known impact craters formed in target rocks with some amount of sediment or sedimentary rock. We have started to explore, using numerical models, the relationship between sediment thickness and final complex crater morphology for impacts into mixed sedimentary and crystalline targets [1]. However, the strength model used in this initial study assumes that the sedimentary material is entirely isotropic [2], and fails to account for the inherent anisotropy of stratified sedimentary rocks. Layered materials are often transversely isotropic, implying that material properties, such as strength, are different in the plane-parallel and plane-perpendicular directions, as shown in Figure 1. Past experiments have analyzed the deformation and failure of numerous transversely isotropic materials, such as shale [e.g., 3] and clays [e.g., 4], which has allowed for constitutive models for anisotropic materials to be developed and algorithms created to be incorporated into modern hydrocodes [5].

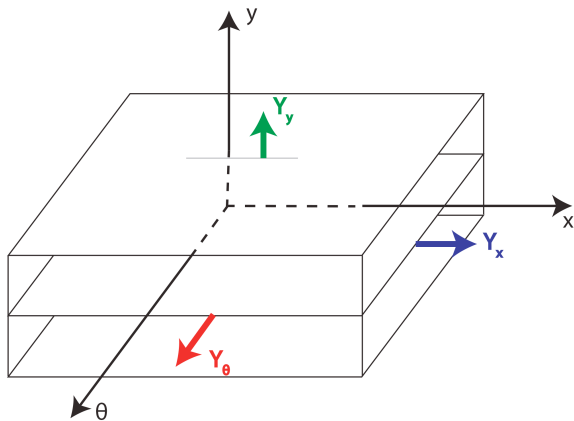


Figure 1: Depiction of a cell of an anisotropic material. The principal axes for simulations conducted in 2D cylindrically symmetric case are indicated by x, y, and θ . The flow stress or material failure strength in each of the principle directions are indicated by Y_x , Y_y and Y_θ [5].

In this abstract, we outline proposed adjustments to the strength model currently used in iSALE to account for transversely isotropic materials, based on algorithms developed by Anderson et al. [5]. We then explore the effect(s) that this implementation has on the

more simple layered sedimentary/crystalline model described in [1].

Hydrocode Simulations: Impacts into mixed sedimentary and crystalline targets were simulated using the multi-rheology hydrocode iSALE-2D [6]. The target was composed of two materials: a crystalline basement overlain by a sedimentary layer of varying thickness. Both the impactor and crystalline basement were composed of granite, using the ANEOS equation of state (EoS) [7] parameters given in [8]. For the sedimentary layer, the Tillotson EoS [9] for limestone was used. For both layers, strength parameters described in [10] were used. The block acoustic fluidization model was used to account for temporary strength loss of the target material [e.g., 11], with parameters similar to those in [12]. Initial results for an isotropic sedimentary layer were presented in [1]. The parameters for the model from the previous work will be kept identical, except for changes to the current stress calculations to account for transverse isotropy.

Implementing Anisotropy: To implement material anisotropy into iSALE, elements of an algorithm developed by Anderson et al. [5] are used, reduced to the simpler 2D cylindrically symmetric case.

Yield Strength Surface. The first step of our modifications to iSALE is to account for anisotropy of yield strength, which is achieved by implementing a modified Tsai-Hill yield criterion [13,14,5]. In this approach a scalar measure of differential stress f_{TH} is defined as:

$$f_{TH} = \frac{1}{6} \left[H (\sigma_{xx} - \sigma_{yy})^2 + G (\sigma_{xx} - \sigma_\theta)^2 + F (\sigma_{yy} - \sigma_\theta)^2 + 2N \sigma_{xy}^2 \right] \quad (1)$$

where σ_{ij} are the components of the stress tensor, and the constants F - H and N are related to the material yield strength in the three material directions Y_x , Y_y , and Y_θ , and the shear strength Y_{xy} by:

$$\frac{G+H}{2} = \left(\frac{Y}{Y_x}\right)^2, \quad \frac{F+H}{2} = \left(\frac{Y}{Y_y}\right)^2, \quad \frac{F+G}{2} = \left(\frac{Y}{Y_\theta}\right)^2, \quad N = \left(\frac{Y}{Y_{xy}}\right)^2 \quad (2)$$

and Y is some reference yield strength. f_{TH} is then used in the same way as the second invariant of the stress tensor in iSALE's plasticity algorithm [2]. I.e., if the $\sqrt{f_{TH}} > Y$ yielding occurs, some of the strain is plastic, and the stresses must be reduced back to the yield surface. Otherwise, stresses lie beneath the yield surface, all strains are elastic, and the computed stresses are carried to the next time step.

In the isotropic case, $Y_x = Y_y = Y_\theta = Y$, implying $F = G = H = 1$, and $Y_{xy} = Y/\sqrt{3}$, implying $N = 3$, and f_{TH} reduces to the familiar second invariant of the devia-

toric stress tensor, J_2 . Under these assumptions, the orientation of the material has no influence on the yield surface (Fig. 2).

In the transversely isotropic case, with bedding planes perpendicular to the y -direction and $Y_y \neq Y_x = Y_\theta = Y$, $F = H = (Y/Y_y)^2$ and $G = 2 - F$. N is given as above. Under these assumptions, the yield surface is equal to Y when the bedding planes of the sedimentary material are oriented vertically (parallel to the y -direction) and, depending on the values of F and N , can vary substantially as a function of bedding plane orientation between horizontal and vertical (Fig. 2).

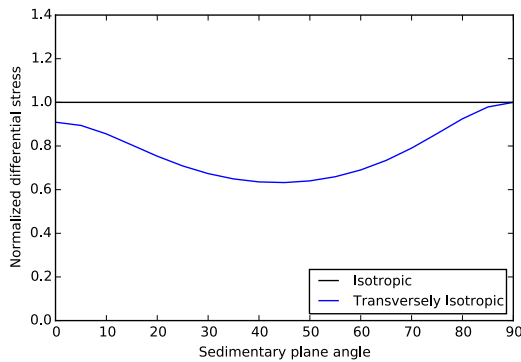


Figure 2: Normalized differential stress (Y/f_{TH}) versus sedimentary plane angle (relative to the horizontal) for a triaxial stress scenario with $\sigma_{yy} < \sigma_{xx} = \sigma_\theta$ and $\sigma_{xy} = 0$. In the isotropic case (black line), the yield curve is independent of bedding plane orientation; in the transverse isotropic case with $Y_y = Y/1.1$ and $Y_{xy} = Y/3$ (blue), the yield curve has a minimum at a bedding orientation of $\sim 45^\circ$.

Material rotation The modified yield criterion described above accounts for anisotropy of strength assuming that the material axes are aligned with the system axes at the beginning of the calculation and remain so throughout the simulation. In dynamic impact simulations this is not a valid assumption. An additional modification is therefore required to track the orientation of the bedding planes in the simulation and to rotate the stress tensor into the material coordinate frame (and back again) when applying the yield criterion.

Initial Results of Hydrocode Modelling: Simulations using the isotropic strength model exploring the effect of sediment thickness on crater size are shown in Figure 3 [1]. For both a porous and non-porous upper layer, when the sediment layer is thin (0-300 m), the weaker sedimentary layer has little influence on final crater radius (~ 7.1 km). As sediment thickness is increased, it resulted in a larger final crater radius (~ 8.7 km). The final crater radius plateaus after a sediment thickness increases beyond 1500 m.

Discussion and Future Work: The thickness of a sedimentary layer above a crystalline basement affects the final crater diameter to a large degree. The sedimentary layer appears to be excavated more efficiently than the crystalline layer. As sedimentary thickness continues to increase, the impactor fails to excavate the crystalline basement, and the final crater radius begins to plateau.

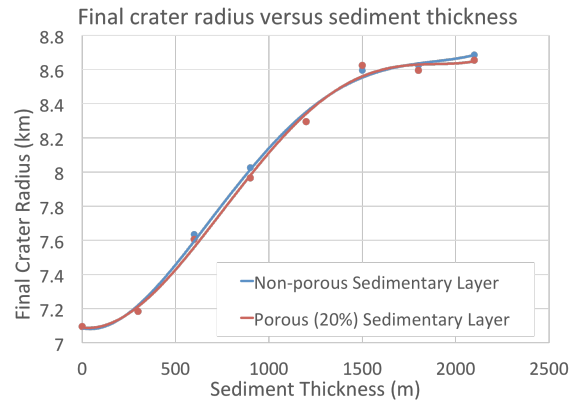


Figure 3: Final crater radius as a function of sediment thickness for non-porous and porous sediment layers. When the sediment layer is thin (0-300 m), the addition of the limestone layer makes little difference. As the sediment layer increases (600-1500 m), the final crater radius increases steadily, before plateauing at a final crater radius of approximately 8.5 km.

Further work will focus on the implementation of the strength model described above. The strength of the sedimentary layer appears to have a significant effect on the final crater morphology. Therefore, it can be expected that changing the model used to describe strength will also have an effect on the crater morphology. We will therefore attempt to determine the effect that transverse isotropy will have on final crater radius.

Acknowledgements: We gratefully acknowledge the developers of iSALE, including Gareth Collins, Kai Wünnemann, Dirk Elbeshausen, Boris Ivanov, and Jay Melosh.

References: [1] Hopkins R. and Osinski G. (2015) *LPSC* 46, 1659. [2] Collins G. et al. (2004) *Meteorit. & Planet. Sci.*, 39(2), 217-31. [3] Niandou H. et al. (1997) *Int. J. Rock Mech. Min. Sci.* 34(1), 3-16. [4] Boehler J. and Sawczuk A. (1977) *Acta Mech.*, 27, 185-206. [5] Anderson C. et al. (1994) *Comput. Mech.*, 15, 201-23. [6] Wünnemann K. et al. (2006) *Icarus*, 180, 514-527. [7] Thomson S. L. and Lauson H. S. (1974). *Report SC-RR-71 0714*, Sandia National Lab., Albuquerque, NM. [8] Pierazzo E. (1997) *Icarus*, 127, 408-23. [9] Tillotson K. H. (1962) *Report GA-3216*, General Atomic, San Diego, CA. [10] Collins G. S. et al. (2008) *Meteorit. & Planet. Sci.*, 43, 1955-77. [11] Wünnemann K. and Ivanov B. A. (2003) *Solar System Research*, 51, 831-845. [12] Goldin T. J. et al. (2006) *Meteorit. Planet. Sci.*, 41(12), 1947-58. [13] Hill R. (1948) *Proc. Roy. Soc. Lond.*, 193: 281-297. [14] Tsai S. W. and Hahn H. T. (1980) *Technomic Publishing Co.*, Lancaster, PA.